

PCCP

Accepted Manuscript



This is an *Accepted Manuscript*, which has been through the Royal Society of Chemistry peer review process and has been accepted for publication.

Accepted Manuscripts are published online shortly after acceptance, before technical editing, formatting and proof reading. Using this free service, authors can make their results available to the community, in citable form, before we publish the edited article. We will replace this *Accepted Manuscript* with the edited and formatted *Advance Article* as soon as it is available.

You can find more information about *Accepted Manuscripts* in the [Information for Authors](#).

Please note that technical editing may introduce minor changes to the text and/or graphics, which may alter content. The journal's standard [Terms & Conditions](#) and the [Ethical guidelines](#) still apply. In no event shall the Royal Society of Chemistry be held responsible for any errors or omissions in this *Accepted Manuscript* or any consequences arising from the use of any information it contains.

Cite this: DOI: 10.1039/c0xx00000x

www.rsc.org/xxxxxx

ARTICLE TYPE

Organic soluble and uniform film forming oligoethylene glycol substituted BODIPY small molecules with improved hole mobility†

Saumya Singh,^{a,b,c} Vijay Venugopalan^{a,c} and Kothandam Krishnamoorthy^{a,b,c,d*}

Received (in XXX, XXX) Xth XXXXXXXXXX 20XX, Accepted Xth XXXXXXXXXX 20XX

DOI: 10.1039/b000000x

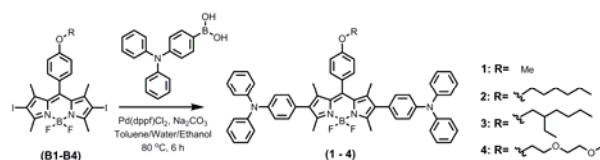
Judiciously chosen side chains of conjugated molecules have positive impact on charge transport properties while used as active material in organic electronic devices. Amongst the side chains, oligoethylene glycols (OEGs) have been relatively unexplored due to its hydrophilic nature. OEGs also affect the smooth film formation of conjugated molecules, which precludes the device fabrication. However, X-ray diffraction studies have shown that OEGs facilitate intermolecular contact, which is a desirable property for the fabrication of organic electronic devices. Thus the challenge is to design and synthesize organic solvent soluble and uniform film forming conjugated molecules with OEG side chains. We have designed and synthesized conjugated small molecules (CSMs) comprising BODIPY as acceptor and triphenylamine as donor with OEG side chain. This molecule forms smooth films while processed from organic solvents. In order to understand the impact of OEG side chain, we have also synthesized alkyl chain analogs. All the molecules exhibit exactly same HOMO and LUMO energy levels, but the packing in solid state is different. CSM with methyl side chain exhibit a inter planar distance of 4.15 Å. Contrary to this, OEG side chain containing CSM showed inter planar spacing of 4.30 Å, which is 0.2 Å less than the alkyl side chain comprising CSMs. Please note that the length of hydrophobic and hydrophilic side chain is same. Interestingly, the OEG side chain comprising CSM showed two orders of higher hole carrier mobilities compared to all the other derivatives. The same molecule also showed extremely low threshold voltage of -0.27 V indicating the OEG side chains' favourable interaction between substrate as well as between molecules.

Introduction

Solution processability of conjugated polymers (CPs) is one of the vital steps in simplifying the fabrication of organic electronic devices. Linear and branched alkyl chains are widely used to solubilise CPs in common organic solvents.¹ Although the alkyl chains increase the solubility, they impact the device efficiency of CPs due to its insulating nature.² Furthermore, alkyl chains affect the packing and thin film morphology of CPs.³ Thus, identification of suitable alkyl chain that positively impacts both solubility and device efficiency is an art.⁴ In case of branched alkyl chain substituted CPs, the branching point also plays decisive role and impact the device efficiency.⁵ Recently, alkyl chains comprising siloxane terminals have been shown to assist packing in CPs and improve device efficiency.⁶

Oligoethylene glycol (OEG) side chains are widely used to synthesize water soluble polymers. However, OEG containing CPs are rare and its use in organic electronic devices are seldom attempted.⁷ The possible reasons are the poor film formation due to decreased glass transition temperature and water solubility of OEG substituted CPs.⁸ To circumvent this issue amphiphilic CPs

45



Scheme 1 Synthesis of BODIPY small molecules (1-4) were synthesized.⁹ In this case, it is difficult to understand the impact of OEG on the device efficiency due to the presence of alkyl chain. Furthermore, amphiphilic molecules form self assembled nanostructures hindering the smooth film formation.^{9b,10} Despite all these drawbacks, an important finding that is relevant for organic electronic devices was reported recently.¹¹ OEG side chains facilitate better interaction between the conjugated backbones.^{9b,11} From the above discussion, it is clear that OEG side chains substituted molecules are preferable, provided the molecules form good films and soluble in organic solvents. A systematic study involving molecules comprising alkyl chain and OEG side chain would provide vital information on the possibility of using OEG as solubilising moiety.

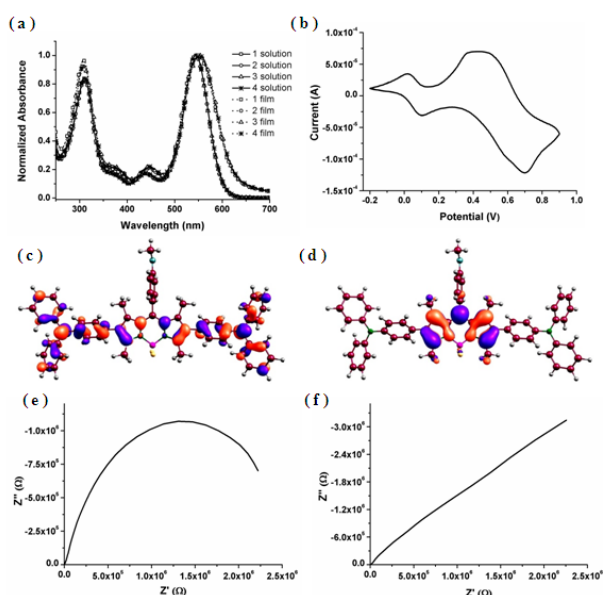


Fig. 1 (a) UV-vis Absorption spectra of **1-4**. (b) Cyclic voltammogram of **3** with ferrocene as internal standard. (c) Surface plots of **1**, HOMO (c) and LUMO (d). Impedance spectra of **4** at 0 V (e) and 0.6 V (f).

Conjugated small molecules (CSMs) can be synthesized with precise molecular weight and without end group contaminations that make them attractive candidates over its polymeric counterparts.¹² Linear and branched alkyl chains are used to solubilise CSMs in common organic solvents.¹³ Recently, we found that triphenylamine containing *i*-indigo CSMs dissolve in common organic solvents while substituted with a butyl chain.¹⁴ We attributed the increase in solubility to the presence of propeller type triphenylamine because having a branched alkyl chain is a must to solubilise *i*-indigo containing small molecules and polymers.¹⁵ With this information in hand, we decided to synthesize OEG containing CSMs with triphenylamine as one of the components. We also synthesized CSMs with linear and branched alkyl chain as solubilising groups. In addition, a CSM containing methyl group was synthesized (Scheme 1). Usually, the shortest side chain (methyl or methoxy) substituted CSMs and polymers are insoluble. Here, the use of triphenylamine as a component of CSMs becomes handy and solubilises CSMs with methyl moiety. The CSMs comprise 4,4-Difluoro-4-borata-3a-azonia-4a-aza-s-indacene (BODIPY) as electron poor and triphenylamine as electron rich moieties. BODIPY has been chosen due to the molecular dipole (3.38–4.12 Debye) that

facilitates strong dipolar interactions and impacts crystallinity and morphology.¹⁶ The charge carrier mobility of the CPs comprising BODIPY have been found to vary from 1×10^{-9} to 1×10^{-3} cm^2/Vs .¹⁷ Very recently, charge carrier mobility of $0.1 \text{ cm}^2/\text{Vs}$ has been achieved by removing the methyl groups in the β position of the pyrrole ring of the BODIPY.¹⁶ In our design, we adhere to the conventional BODIPY core because modulation in the methyl groups at either α or β positions can compromise the optical properties, albeit it may increase charge carrier mobility.^{16,18} Furthermore, BODIPY comprising CPs have been explored as donor in organic solar cells due to excellent optical properties, negligible triplet state formation and photostability.¹⁹ Thus an approach that can modulate the charge carrier transport of BODIPY based CSMs would impact the ultimate objective of fabrication of efficient organic solar cells. Towards this objective, we have fabricated field effect transistors (FET) and studied all the device metrics to understand the effect of nature of the side chain. We also studied the response of the CSMs as function of alternating current (AC) due to the presence of dipoles in these molecules.

Results and Discussion

BODIPY containing CSMs were synthesized by carrying out Suzuki coupling between boronic acid substituted triphenylamine and diiodoBODIPY (Scheme 1).²⁰ The diiodoBODIPY was synthesized by condensing 2,4-dimethylpyrrole with corresponding aldehydes.^{17a,21} The UV-vis absorption spectra of the CSMs were recorded using chloroform as solvent. The absorption spectra exhibit two clear global maxima with a high energy peak at 310 nm and low energy peak at 545 nm (Fig. 1a). The 310 nm and 545 nm peaks arise from the triphenylamine moieties and BODIPY, respectively.²² All the CSMs exhibit exactly same absorption profiles indicating that the side chain has no effect on the energy levels and packing behavior in solution. The UV-vis absorption spectra of thin films of the CSMs were recorded using quartz plates as substrates. The low energy absorption maximum was found to bathochromic shift by 7 nm, which indicates better packing of the CSMs in thin films. It must be noted that the side chains have no impact on optical characteristics of the CSMs. We will discuss more on this in the X-ray diffraction studies (*vide infra*). The onset of the low energy peak was used to calculate the band gap of CSMs and was found to be 2 eV (Table 1). To determine the band edges of the CSMs, cyclic voltammetry was recorded using CSMs coated Pt wire as working electrode, Ag/Ag^+ as reference electrode and Pt foil as

Table 1 Electrochemical, optical and thermal data of CSMs

CSMs	$E^{\text{ox, onset}}$ (V)	$E^{\text{red, onset}}$ (V)	HOMO ^{cl} (eV)	LUMO ^{cl} (eV)	E_g^{cl} (eV)	λ_{onset}	E_g^{opt} (eV)	T_g (°C)	T_c (°C)	T_m (°C)
1	0.38	-1.38	-5.12	-3.36	1.76	626	1.98	-	-	-
2	0.41	-1.32	-5.15	-3.42	1.73	626	1.98	93	-	268
3	0.40	-1.34	-5.14	-3.40	1.74	628	1.97	92	-	254
4	0.39	-1.32	-5.13	-3.42	1.71	629	1.97	103	174	254

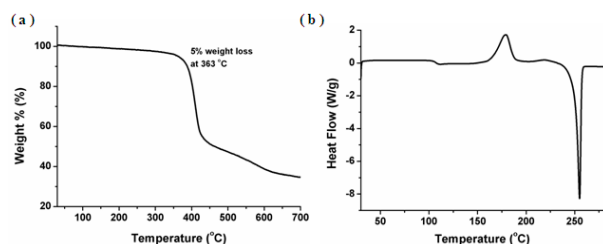


Fig. 2 Thermogram (a) and differential scanning calorimetry curve (b) of **4**.

counter electrode. The cyclic voltammograms (CVs) were recorded by sweeping the working electrode potential in the anodic and cathodic segments in 0.1 M tetrabutylammonium hexafluorophosphate in acetonitrile. The separate sweeps were recorded to avoid prepeaks that were observed in the CVs of conjugated molecules. We also recoded the whole sweeps between -2 V and 0.8 V vs Ag/Ag^+ . Please note that the CSMs are insoluble in acetonitrile, thus it was possible to record cyclic voltammogram of thin films. During the anodic and cathodic sweeps of **1-3**, the peak current increased upon increase in number of cycles and stabilized after 10 cycles (Fig. S24, ESI†). In case of **4**, there was no appreciable change in the current while recording the CV in absence of ferrocene as internal standard. However, we did notice a small decrease upon cycling and then the current stabilized. If there was degradation of CSMs, the peak current would have continued to decrease drastically. However, that is not the case, hence the CSMs are redox stable. In the anodic scan, oxidation of the CSMs starts around 0.4 V vs Ag/Ag^+ and in the reverse scan corresponding reduction peak was observed (Fig. 1b). The ΔE_p was found to be higher than 59 mV indicating the redox process is quasi reversible (the ΔE_p and peak current ratios are provided in Table S1, ESI†). In the cathodic sweep, the reduction peak was observed around -1.3 V and corresponding oxidation peak was observed in the reverse scan. This redox process is also quasi reversible (the ΔE_p and peak current ratios are provided in Table S1, ESI†). To determine the frontier orbital energy level, ferrocene was added in the last sweep. The band edges with respect to vacuum level were determined by calibrating the oxidation and reduction of CSMs with respect to ferrocene using the formula $\text{HOMO} = -(E_{\text{ox/onset}} + 4.8)$ eV.^{17a,21f,23} The band edges are provided in Table 1. The HOMO energy level of all the CSMs is around -5.2 eV, which is very close to the energy level of oxygen.²⁴ Density functional theory calculations were carried out to understand the distribution of wave function in the CSMs. B3LYP functional and 6-31g* basis set was used to determine the energy levels.^{17a,21f,25} The surface plots are shown in Fig. 1 and Fig. S15 ESI†. The surface plots indicate that the HOMO wave function is distributed over the whole molecule (Fig. 1c). On the other hand, the LUMO wave function resides exclusively on the BODIPY moiety (Fig. 1d). Similar trend was observed in triphenylamine containing small molecules.¹⁴ The CSMs has a permanent dipole, which is unique compared to other conjugated molecules, hence their response to alternating current (AC) is likely to be of interest. We used AC impedance spectroscopy to study the electrical characteristics of the CSMs. The experiments

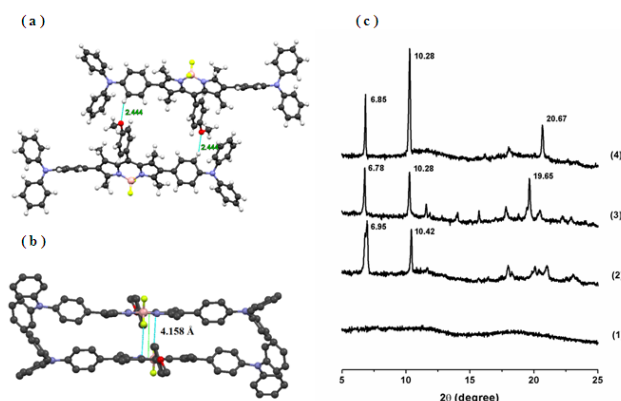


Fig. 3 The crystal structure showing the slip stack of **1** (a) and the inter planar distance (b). The C, O, N, F and B atoms are shown in grey, red, cyan, yellow and pink, respectively. Powder XRD pattern of **1-4** (c).

were done in a conventional three electrode cell by applying potential amplitude of 5 mV and frequency range of 0.01 Hz and 100 kHz.²⁶ The measurements were done at 0 V and 0.6 V. The nyquist plot is a semicircle (0 V) without linear line in the low frequency regime (Fig. 1e), which corresponds to an equivalent circuit comprising a resistor and double layer capacitor connected in parallel.²⁷ The resistance and capacitance arise from the CSMs and its interface with electrolyte and electrode. This parallel circuit is connected in series with another resistor which originates from all external resistances.²⁷ Such a nyquist plot is observed for conjugated polymers in absence of electrolyte.^{27,28} Contrary to this, we observed only linear line while the nyquist plots were recorded at an applied potential of $+0.6$ V indicating pure capacitive behavior (Fig. 1f). Similar trend is observed for graphene based materials and poly(phenylene vinylene) conjugated polymers at 0 V.^{26a,27} It should be noted that the conjugated polymers exhibit semicircle and linear line in presence of electrolyte.²⁹ Thus, the unusual response of CSMs is likely due to the presence of dipole. Thus, the CSMs reported in this paper are likely to be suitable candidates for thin film transistors that respond to frequency.³⁰

The thermal characteristics of the CSMs were studied by thermogravimetric analysis and differential scanning calorimetry. In the thermogram, significant weight loss was not observed till 200 °C for all the CSMs (Fig. 2a). This result indicates that the CSMs can be thermally annealed upto 200 °C without degradation. The DSC data were obtained from the third heating cycle to avoid thermal hysteresis. The DSC curves provided information about the change in glass transition and crystallization temperature. For **1**, the DSC curve was featureless. The T_g of **2** and **3** was found to be around 93 °C, which increased to 103 °C for **4**. This is likely due to increase in interaction between the molecules facilitated by OEG side chain. Transition for crystallization was not observed for **2** and **3**. But, a well defined peak indicating the crystallization was observed for **4** at 174 °C (Fig. 2b). The increased T_g and well defined T_c observed for **4** is an indication of ameliorated interaction between the CSMs. In case of **4**, clear melting transition was also observed at 254 °C. In order to understand the packing pattern, we attempted to grow single crystals of CSMs.³¹ For **1**, we were able to grow

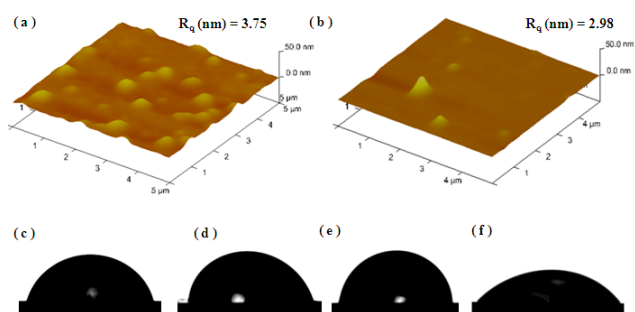


Fig. 4 AFM height images and root mean square roughness (R_q) of thin films of **1** (a) on unmodified SiO_2 substrate, **4** (b) on HMDS modified SiO_2 substrate. CA of **1** (c), **2** (d), **3** (e) and **4** (f) coated on unmodified SiO_2 surface.

single crystals from a binary solvent system of dichloromethane and pet ether and obtained the diffraction pattern. From the single crystal XRD, we could conclude that **1** crystallizes in triclinic crystal system with P-1 space group. The phenyl ring connecting the side chain with BODIPY core is perpendicular to the plane of the conjugated backbone (Fig. 3a). Similarly, the phenyl ring of the triphenylamine is twisted at an angle of 51.1° with respect to the plane of BODIPY. During the stacking process, the molecules slip to accommodate the twisted phenyl rings (Fig. 3a). To calculate the interplanar distance, least square plan was drawn connecting 26 atoms. The distance between the two backbones is found to be 4.15 \AA (Fig. 3b). Unfortunately, all our attempts to prepare single crystals of other molecules were unsuccessful. Although we were able to get crystals, they were not large enough to mount on the single crystal XRD instrument. Thus, we recorded thin film XRD of all the samples. Surprisingly, thin film XRD pattern of **1** didn't show any peak indicating phase transition while preparing films. Contrary to this, sharp peaks were observed for **2**, **3** and **4** (Fig. 3c). From the d spacing calculated for **1** and the similar structure of **2**, **3** and **4** we can assume that the inter planar spacing will be around 4 \AA for the CSMs. For **3** and **4**, sharp peaks were observed at a 2θ of 19.6° and 20.6° , which corresponds to a d spacing of 4.51 and 4.30 \AA , respectively. From the single crystal and thin film XRD data, the d spacing is shortest for methyl group substituted CSMs (**1**) and the longest for alkyl chain substituted CSMs (**3**). Although, OEG (**4**) and alkyl chains (**3**) are of almost same length, the interplanar

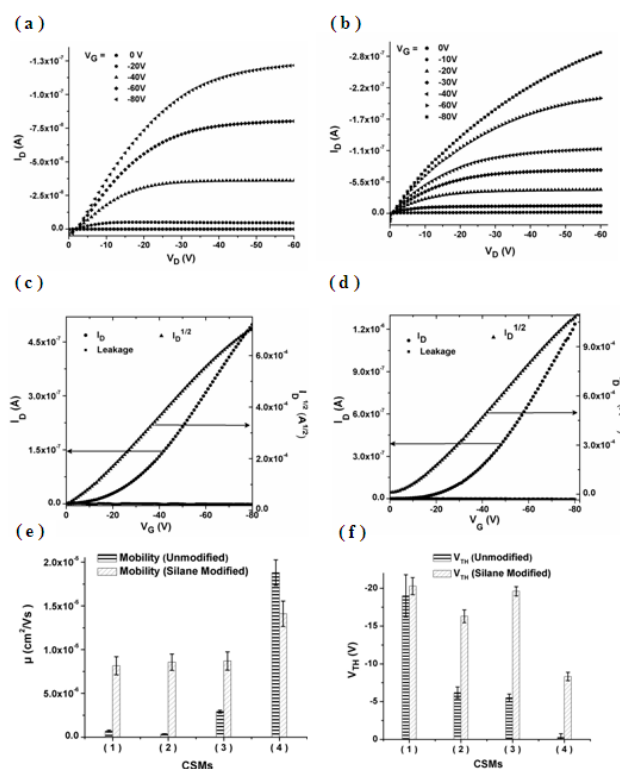


Fig. 5 Output characteristic curves of **3** (a) and **4** (b) using unmodified FET Substrate. Transfer characteristic curves of **4** (c) using unmodified and **4** (d) using HMDS modified substrate. Bar graph showing the hole carrier mobility (e) and threshold voltage (f) of CSMs with error bars.

spacing for **4** is closer to **1**. Thus, the OEG side chain facilitates better interaction between CSMs. It should be recalled that the side chain didn't alter the optical properties of the CSMs (Fig. 1a), but the packing behavior is different as determined by XRD studies. Similar characteristics were observed for small molecules and polymers containing linear and branched alkyl chains.^{3c,d}

Thin film morphology of the CSMs was studied using SiO_2 grown silicon substrates. The SiO_2 surface is hydrophilic. To impart hydrophobicity to this surface, a monolayer of hexamethyldisilazane (HMDS) was prepared. Both types of substrates were used to prepare thin films of CSMs. We chose

Table 2 OFET device metrics of CSMs 1-4

CSMs	μ (cm^2/Vs) ^a	V_T (V) ^a	$I_{\text{on/off}}$ ^{a*}	g_m (nS) ^a	μ (cm^2/Vs) ^b	V_T (V) ^b	$I_{\text{on/off}}$ ^{b*}	g_m (nS) ^b
1	6.80E-07	-19	1.3×10^3	0.55	8.16E-06	-20.3	9.2×10^3	12.8
2	3.50E-07	-6.2	1.5×10^3	0.26	8.57E-06	-16.3	5.3×10^4	14
3	2.91E-06	-5.5	1.7×10^3	5.2	8.70E-06	-19.6	3.1×10^4	16
4	1.88E-05	-0.27	7.5×10^2	37.3	1.41E-05	-8.33	9.0×10^3	26.1

a – Unmodified SiO_2 substrate, b – HMDS modified SiO_2 substrates, *- calculated from semi logarithmic plot of I_D vs V_G (ref 34)

these substrates for morphological studies because same substrates were used for the fabrication of FETs. For **1**, the films prepared on both modified and unmodified SiO₂ have troughs and crests indicating a rough surface with high rms values (Fig. 4a). For **2** and **3**, the films were uniform without apparent troughs and crests indicating formation of very smooth film with low rms values. We observed different morphological features for **4**. Thin film of **4** was found to be very smooth in unmodified substrate. Contrary to this, the morphology of **4** prepared on HMDS modified surface was rough, which is due to the incompatibility between hydrophilic OEG substituted BODIPY (**4**) and hydrophobic HMDS modified substrate (Fig. 4b). Water drop contact angle (CA) was also used to understand the surface wettability of the films. This experiment shed more light on the surface property of thin films of CSMs, in this particular instance due to the variation in lipophilic nature of side chains. The CA was found to be 79°, 82° and 86° for **1**, **2** and **3**, respectively (Fig. 4c, d, and e). On the other hand, the CA for **4** was significantly lower (49°) (Fig. 4f) because of the presence of hydrophilic OEG side chain. The same measurements were repeated with HMDS modified substrates. In this case, the CA for **1**, **2** and **3** was found to be 106°, 103° and 109°, respectively (Fig. S17, ESI†). The close CA values of these films are due to similar morphology and the surface functionalities. Interestingly, the CA for **4** increased from 49° to 100°. The difference is due to the change in morphology from a smooth film to a rough surface while modifying the base substrate with HMDS. The HMDS imparts hydrophobic character to the substrate, which is not compatible to the hydrophilic side chain of **4** leading to a rough morphology. Increase in surface roughness increases the CA,³² which is the reason for higher CA of **4**.

Next, we fabricated field effect transistors using SiO₂ as gate dielectric, heavily n doped Si as gate and gold as source and drain electrodes. The gate as well as source and drain contacts were at the bottom with the semiconducting CSMs at the channel. The width of the channel was 1mm and the length was varied between 2.5 μ to 10 μ. The variation in length didn't impact OFET device metrics. We fabricated two types of devices, (i) without silane (HMDS) modification and (ii) with silane modification. Conventionally, enhancement in hole carrier mobility has been attributed to hydrophobic silanes.³³ Furthermore, in our experiments the **1**, **2** and **3** may have favorable interaction with the HMDS modified surface. Contrary to this, compound **4** may have favorable interaction with the unmodified surface. The CSMs were spun on top of the substrates from chloroform solutions. The device fabrication and measurements were carried out inside argon filled glove box. Output characteristic curves were recorded while sweeping the drain voltage (V_D) between 0 and -60V and applying a constant gate voltage (V_G). The output characteristic curves showed typical linear and saturation regimes with a good gate modulation as a function of applied gate voltage (V_G). The linear regime for **1**, **2** and **3** didn't start at 0V, which is likely due to the presence of trap states at the CSM dielectric interface (Fig. 5a). Contrary to this, the linear regime for **4** started at 0 V (Fig. 5b). The device metrics are shown in Table 2. Hole carrier mobilities are calculated using the standard saturation regime quadratic model equation $\mu = I_{DS}/(V_{GS}-V_{th})^2 \times 2L/WC_{OX}$. Transconductance (g_m) is calculated in the saturation regime with

a constant V_{DS}, which is given as $(\partial I_{DS}/\partial V_{GS})|_{V_{DS}}$, and the inverse sub-threshold swing is calculated from the slope inverse of Log(I_{DS}) Vs (V_{GS}) plot. The I_{on}/I_{off} was calculated from the semi logarithmic plot of I_D vs V_G (Fig. S20 and Fig. S21, ESI†).³⁴ The hole carrier mobility (μ) calculated for **4** was found to be two order higher than other CSMs. From the XRD data analysis, we know that CSMs **1** and **4** are closely packed than **2** and **3**. However, **1** doesn't form smooth film which results in poor charge carrier mobility. On the other hand, **4** forms a good film, hence the mobility is increased by two orders. Thus, the higher mobility of **4** is due to the combination of close packing and smooth film formation. It is also worth noting that the threshold voltage (V_{th}) is -0.27 V for **4** (Fig. 5c), which is at least an order lower than the other CSMs. The transconductance (g_m) is the highest (37 nS) for **4** congruent with the high hole mobility observed. However the sub-threshold slope of all molecules is comparable indicating a similar distributions of deep trap states. All these indicate that the OEG side chain facilitates interaction with the dielectric surface and between the molecules. In the HMDS modified devices, the charge carrier mobility increased by two to nine times for **1**, **2** and **3**. This is anticipated due to the hydrophobicity of the gate dielectric surface, which lead to better interaction between the gate dielectric and CSMs. Contrary to this, the hole mobility is almost unaffected in case of **4**. However it must be noted that the improved mobility values for HMDS modified **1**, **2** and **3** are still considerably lower than the mobility values observed for **4**. Representative transfer characteristic curve is shown in Fig. 5d and the other output and transfer characteristic curves are shown in Fig. S18, ESI†. Interestingly thermal and solvent annealing didn't affect the device efficiencies for all molecules.

90 Summary

In summary, we have designed and synthesized CSMs with a propeller type triphenylamine as donor and BODIPY as acceptor. The triphenylamine enhances the solubility of the CSMs in organic solvents. In fact, a CSM with OEG side chain was found to be soluble in common organic solvents. The OEG comprising CSM exhibit high glass transition temperature and forms smooth films while processed from organic solvents. The OEG facilitate better intermolecular contact, which lead to OFETs with superior device efficiencies. The threshold voltage was as small as -0.27 V and the hole carrier mobility was 1.8 x 10⁻⁵ cm²/Vs, which is comparable to regioregular polythiophene substituted with OEG side chain (3.5 x 10⁻⁵ cm²/Vs).⁸ The understanding emanated from this work opens up the possibility of exploring OEG side chains with other conjugated molecules for the fabrication of organic electronic devices.

Acknowledgements

We thank CSIR for funding (TAPSUN NWP 54). S. S thank UGC for fellowship. We thank Dr Nithyanandhan for discussion, Mr Puneet Khandelwal and Dr Pankaj Poddar for AFM images. We also thank Mr Tanay Kundu and Dr Rahul Banerjee for single crystal XRD measurements.

Notes and references

- ^a Polymer Science and Engineering Division, CSIR-National Chemical Laboratory-Pune, Pune, Maharashtra, India 411008 Tel: +91-20-25903075; E-mail: k.krishnamoorthy@ncl.res.in
- ^b Academy of Scientific and Innovative Research, New delhi, India
- ^c CSIR-Network of Institutes for Solar Energy, New Delhi
- ^d Center of Excellence in Surface Science, CSIR-National Chemical Laboratory-Pune, Pune, Maharashtra, India 411008
- † Electronic Supplementary Information (ESI) available: [Experimental details and figures are available]. See DOI: 10.1039/b000000x/
- (a) Y.-J. Cheng, S.-H. Yang and C.-S. Hsu, *Chem. Rev.*, 2009, **109**, 5868–5923; (b) T. Lei, J.-Y. Wang and J. Pei, *Chem. Mater.*, DOI: 10.1021/cm4018776; (c) J. Mei and Z. Bao, *Chem. Mater.*, 2013, DOI: 10.1021/cm4020805; (d) A. Facchetti, *Chem. Mater.*, 2011, **23**, 733–758; (e) C. Cabanetos, A. E. Labban, J. A. Bartelt, J. D. Douglas, W. R. Mateker, J. M. J. Fréchet, M. D. McGehee and P. M. Beaujuge, *J. Am. Chem. Soc.*, 2013, **135**, 4656–4659.
 - (a) C. Piliago, T. W. Holcombe, J. D. Douglas, C. H. Woo, P. M. Beaujuge and J. M. Fréchet, *J. Am. Chem. Soc.*, 2010, **132**, 7595–7597; (b) A. P. Zoombelt, M. A. M. Leenen, M. Fonrodona, Y. Nicolas, M. M. Wienk and R. A. J. Janssen, *Polymer*, 2009, **50**, 4564–4570.
 - (a) W. P. Hsu, K. Levon, K. S. Ho, A. S. Myerson and T. K. Kwei, *Macromolecules*, 1993, **26**, 1318–1323; (b) P. Keg, A. Lohani, D. Fichou, Y. M. Lam, Y. Wu, B. S. Ong, and S. G. Mhaisalkar, *Macromol. Rapid Commun.*, 2008, **29**, 1197–1202; (c) J. Liu, Y. Zhang, H. Phan, A. Sharenko, P. Moonshin, B. Walker, V. Promarak, T. -Q. Nguyen, *Adv. Mater.* 2013, **25**, 3645–3650; (d) M. S. Chen, O. P. Lee, J. R. Niskala, A. T. Yiu, C. J. Tassone, K. Schmidt, P. M. Beaujuge, S. S. Onishi, M. F. Toney, A. Zettl, J. M. J. Fréchet, *J. Am. Chem. Soc.*, 2013, **135**, 19229–19236.
 - (a) P. M. Beaujuge and J. M. J. Fréchet, *J. Am. Chem. Soc.*, 2011, **133**, 20009–20029; (b) H. Bronstein, D. S. Leem, R. Hamilton, P. Woebkenberg, S. King, W. Zhang, R. S. Ashraf, M. Heeney, T. D. Anthopoulos, J. de Mello and I. McCulloch, *Macromolecules*, 2011, **44**, 6649–6652; (c) I. Osaka, R. Zhang, G. Sauv e, D.-M. Smilgies, T. Kowalewski and R. D. McCullough, *J. Am. Chem. Soc.*, 2009, **131**, 2521–2529.
 - (a) T. Lei, J.-H. Dou and J. Pei, *Adv. Mater.*, 2012, **24**, 6457–6461; (b) I. Meager, R. S. Ashraf, S. Mollinger, B. C. Schroeder, H. Bronstein, D. Beatrup, M. S. Vezie, T. Kirchartz, A. Salleo, J. Nelson and I. McCulloch, *J. Am. Chem. Soc.*, 2013, **135**, 11537–11540; (c) F. Zhang, Y. Hu, T. Schuettfort, C. Di, X. Gao, C. R. McNeill, L. Thomsen, S. C. Mannsfeld, W. Yuan, H. Sirringhaus and D. Zhu, *J. Am. Chem. Soc.*, 2013, **135**, 2338–2349.
 - (a) J. Mei, D. H. Kim, A. L. Ayzner, M. F. Toney and Z. Bao, *J. Am. Chem. Soc.*, 2011, **133**, 20130–20133; (b) J. Lee, A.-R. Han, H. Yu, T. J. Shin, C. Yang and J. H. Oh, *J. Am. Chem. Soc.*, 2013, **135**, 9540–9547; (c) J. Lee, A.-R. Han, J. Kim, Y. Kim, J. H. Oh and C. Yang, *J. Am. Chem. Soc.*, 2012, **134**, 20713–20721.
 - (a) J. Roncali, R. Garreau, D. Delabouglise, F. Garnier and M. Lemaire, *J. Chem. Soc., Chem. Commun.*, 1989, **0**, 679–681; (b) J. Roncali, L.H. Shi and F. Garnier, *J. Phys. Chem.*, 1991, **95**, 8983–8989; (c) L. Holzer, B. Winkler, F. P. Wenzl, S. Tasch, L. Dai, A. W. H. Mau and G. Leising, *Synth. Met.* 1999, **100**, 71–77; (d) F. Huang, Y. Zhang, M. S. Liu and A. K. Y. Jen, *Adv. Funct. Mater.*, 2009, **19**, 2457–2466.
 - M. Shao, Y. He, K. Hong, C. M. Rouleau, D. B. Geohegan and K. Xiao, *Polym. Chem.*, 2013, **4**, 5270–5274.
 - (a) J. Yin, Y. Zhou, T. Lei and J. Pei, *Angew. Chem., Int. Ed.*, 2011, **50**, 6320–6323; (b) J. Mei, K. R. Graham, R. Stalder, S. P. Tiwari, H. Cheun, J. Shim, M. Yoshio, C. Nuckolls, B. Kippelen, R. K. Castellano and J. R. Reynolds, *Chem. Mater.*, 2011, **23**, 2285–2288; (c) M. A. Naik, N. Venkatramaiah, C. Kanimozhi and S. Patil, *J. Phys. Chem. C*, 2012, **116**, 26128–26137.
 - T. Bjørnholm, D. R. Greve, N. Reitzel, T. Hassenkam, K. Kjaer, P. B. Howes, N. B. Larsen, J. Bøgelund, M. Jayaraman, P. C. Ewbank and R. D. McCullough, *J. Am. Chem. Soc.*, 1998, **120**, 7643–7644.
 - C. Kanimozhi, N. Yaacobi-Gross, K. W. Chou, A. Amassian, T. D. Anthopoulos and S. Patil, *J. Am. Chem. Soc.*, 2012, **134**, 16532–16535.
 - (a) J. Roncali, *Acc. Chem. Res.*, 2009, **42**, 1719–1730; (b) B. Walker, C. Kim and T.-Q. Nguyen, *Chem. Mater.*, 2011, **23**, 470–482; (c) Y. Sun, G. C. Welch, W. L. Leong, C. J. Takacs, G. C. Bazan and A. J. Heeger, *Nat. Mater.*, 2012, **11**, 44–48; (d) J. Zhou, X. Wan, Y. Liu, Y. Zuo, Z. Li, G. He, G. Long, W. Ni, C. Li, X. Su and Y. Chen, *J. Am. Chem. Soc.*, 2012, **134**, 16345–16351.
 - (a) O. P. Lee, A. T. Yiu, P. M. Beaujuge, C. H. Woo, T. W. Holcombe, J. E. Millstone, J. D. Douglas, M. S. Chen and J. M. J. Fréchet, *Adv. Mater.*, 2011, **23**, 5359–5363; (b) B. H. Wunsch, M. Rumi, N. R. Tummala, C. Risko, D.-Y. Kang, K. X. Steirer, J. Gantz, M. Said, N. R. Armstrong, J.-L. Br edas, D. Bucknall and S. R. Marder, *J. Mater. Chem. C*, 2013, **1**, 5250–5260; (c) D. Khim, K. -J. Baeg, J. Kim, M. Kang, S. -H. Lee, Z. Chen, A. Facchetti, D. -Y. Kim, Y. -Y. Noh, *ACS Appl. Mater. Interfaces*, 2013, **5**, 10745–10752.
 - S. S. Dharmapurikar, A. Arulkashmir, C. Das, P. Muddellu and K. Krishnamoorthy, *ACS Appl. Mater. Interfaces*, 2013, **5**, 7086–7093.
 - (a) J. Mei, K. R. Graham, R. Stalder and J. R. Reynolds, *Org. Lett.*, 2010, **12**, 660–663; (b) E. Wang, Z. Ma, Z. Zhang, K. Vandewal, P. Henriksson, O. Ingan s, F. Zhang and M. R. Andersson, *J. Am. Chem. Soc.*, 2011, **133**, 14244–14247.
 - H. Usta, M. D. Yilmaz, A.-J. Avestro, D. Boudinet, M. Denti, W. Zhao, J. F. Stoddart and A. Facchetti, *Adv. Mater.*, 2013, **25**, 4327–4334.
 - (a) B. C. Popere, A. M. Della Pelle and S. Thayumanavan, *Macromolecules*, 2011, **44**, 4767–4776; (b) T. Bura, N. Leclerc, S. Fall, P. L eveque, T. Heiser, P. Retailleau, S. Rihn, A. Mirloup and R. Ziessel, *J. Am. Chem. Soc.*, 2012, **134**, 17404–17407; (c) R. Yoshii, H. Yamane, A. Nagai, K. Tanaka, H. Taka, H. Kita and Y. Chujo, *Macromolecules*, 2014, **47**, 2316–2323; (d) A. M. Poe, A. M. D. Pelle, A. V. Subrahmanyam, W. White, G. Wantz and S. Thayumanavan, *Chem. Commun.*, 2014, **50**, 2913–2915.
 - (a) A. Loudet and K. Burgess, *Chem. Rev.*, 2007, **107**, 4891–4932; (b) G. Ulrich, R. Ziessel and A. Harriman, *Angew. Chem., Int. Ed.*, 2008, **47**, 1184–1201; (c) N. Boens, V. Leen and W. Dehaen, *Chem. Soc. Rev.*, 2012, **41**, 1130–1172.
 - (a) T. Rousseau, A. Cravino, T. Bura, G. Ulrich, R. Ziessel and J. Roncali, *Chem. Commun.*, 2009, 1673–1675; (b) T. Rousseau, A. Cravino, E. Ripaud, P. Leriche, S. Rihn, A. De Nicola, R. Ziessel and J. Roncali, *Chem. Commun.*, 2010, **46**, 5082–5084; (c) B. Kim, B. Ma, V. R. Donuru, H. Liu and J. M. J. Fr chet, *Chem. Commun.*, 2010, **46**, 4148–4150; (d) H.-Y. Lin, W.-C. Huang, Y.-C. Chen, H.-H. Chou, C.-Y. Hsu, J. T. Lin and H.-W. Lin, *Chem. Commun.*, 2012, **48**, 8913–8915; (e) M. Shrestha, L. Si, C.-W. Chang, H. He, A. Sykes, C.-Y. Lin and E. W.-G. Diau, *J. Phys. Chem. C*, 2012, **116**, 10451–10460; (f) D. Cortizo-Lacalle, C. T. Howells, S. Gambino, F. Vilela, Z. Vobecka, N. J. Findlay, A. R. Inigo, S. A. J. Thomson, P. J. Skabara and I. D. W. Samuel, *J. Mater. Chem.*, 2012, **22**, 14119–14126.

- 20 (a) S. Zhu, N. Dorh, J. Zhang, G. Vegesna, H. Li, F. -T. Luo, A. 65
Tiwari and H. Liu, *J. Mater. Chem.*, 2012, **22**, 2781–2790; (b)
G. Meng, S. Velayudham, A. Smith, R. Luck and H. Liu,
5 *Macromolecules* 2009, **42**, 1995–2001.
- 21 (a) T. E. Wood and A. Thompson, *Chem. Rev.* 2007, **107**, 70
1831–1861; (b) V. R. Donuru, G. K. Vegesna, S. Velayudham,
S. Green and H. Liu, *Chem. Mater.*, 2009, **21**, 2130–2138; (c) C.
10 Thivierge, A. Loudet and K. Burgess, *Macromolecules*, 2011,
44, 4012–4015; (d) Y. Cakmak and E. U. Akkaya, *Org. Lett.*,
2009, **11**, 85–88; (e) Y. Hayashi, N. Obata, M. Tamaru, S.
15 Yamaguchi, Y. Matsuo, A. Saeki, S. Seki, Y. Kureishi, S. Saito,
S. Yamaguchi and H. Shinokubo, *Org. Lett.*, 2012, **14**,
866–869; (f) B. C. Popere, A. M. Della Pelle, A. Poe, G. Balaji
and S. Thayumanavan, *Chem. Sci.*, 2012, **3**, 3093–3102.
- 22 H. Zhao, B. Wang, J. Liao, H. Wang, and G. Tan, *Tetrahedron 80*
Lett., 2013, **54**, 6019–6022.
- 23 A. Kumar, J. G. Bokria, Z. Buyukmumcu, T. Dey and G. A.
Sotzing, *Macromolecules*, 2008, **41**, 7098–7108.
- 24 (a) B. C. Thompson, Y.-G. Kim and J. R. Reynolds,
20 *Macromolecules*, 2005, **38**, 5359–5362; (b) D. M. de Leeuw, M.
M. J. Simenon, A. R. Brown and R. E. F. Einerhand, *Synth.* 85
Met., 1997, **87**, 53–59.
- 25 S. K. Sarkar and P. Thilagar, *Chem. Commun.*, 2013, **49**, 8558–
8560.
- 26 (a) M. F. El-Kady and R. B. Kaner, *Nature Commun.*, 2013, **4**, 90
1–9; (b) L. Pan, G. Yu, D. Zhai, H. R. Lee, W. Zhao, N. Liu, H.
Wang, B. C. -K. Tee, Y. Shi, Y. Cui and Z. Bao, *Proc. Natl.*
Acad. Sci. U.S.A. 2012, **109**, 9287–9292.
- 27 A. Munar, A. Sandström, S. Tang and L. Edman, *Adv. Funct.*
30 *Mater.*, 2012, **22**, 1511–1517.
- 28 B. W. Johnson, D. C. Read, P. Christensen, A. Hamnett and R. 95
D. Armstrong, *J. Electroanal. Chem.* 1994, **364**, 103–109.
- 29 (a) M. Meier, S. Karg and W. Riess, *J. Appl. Phys.*, 1997, **82**,
1961–1966; (b) T. Stöcker, A. Köhler and R. Moos, *J. Polym.*
35 *Sci., Part B: Polym. Phys.*, 2012, **50**, 976–983; (c) R. Y.
Mahale, A. Arulkashmir, K. Dutta and K. Krishnamoorthy,
Phys. Chem. Chem. Phys., 2012, **14**, 4577–4583; (d) T. F. Otero
and E. de Larreta, *J. Electroanal. Chem.*, 1988, **244**, 311–318.
- 30 D. R. Lenski, A. Southard and M. S. Fuhrer, *Appl. Phys. Lett.*, 100
2009, **94**, 232103-1–232103-3.
- 31 (a) R. Fitzner, E. Mena-Osteritz, A. Mishra, G. Schulz, E.
Reinold, M. Weil, C. Köhner, H. Ziehlke, C. Elschner, K. Leo,
M. Riede, M. Pfeiffer, C. Uhrich and P. Bäuerle, *J. Am. Chem.*
45 *Soc.*, 2012, **134**, 11064–11067; (b) Z. Cai, Y. Guo, S. Yang, Q.
Peng, H. Luo, Z. Liu, G. Zhang, Y. Liu and D. Zhang, *Chem.*
Mater., 2013, **25**, 471–478; (c) G. Balaji, M. Parameswaran, T.
M. Jin, C. Vijila, Z. Furong and S. Valiyaveetil, *J. Phys. Chem.*
C, 2010, **114**, 4628–4635.
- 32 (a) H. Y. Erbil, A. L. Demirel, Y. Avci and O. Mert, *Science* 105
2003, **299**, 1377–1380; (b) L. Jiang, Y. Zhao and J. Zhai,
50 *Angew. Chem., Int. Ed.* 2004, **43**, 4338–4341.
- 33 Y. Wen, Y. Liu, Y. Guo, G. Yu and W. Hu, *Chem. Rev.*, 2011,
111, 3358–3406.
- 34 (a) O. Knopfmacher, M. L. Hammock, A. L. Appleton, G.
55 Schwartz, J. Mei, T. Lei, J. Pei and Z. Bao, *Nat. Commun.*
2014, **5**, 3954/1-3954/9; (b) S. Kobayashi, T. Nishikawa, T.
Takenobu, S. Mori, T. Shimoda, T. Mitani, H. Shimotani, N. 110
Yoshimoto, S. Ogawa and Y. Iwasa, *Nat. Mater.*, 2004, **3**, 317–
322.

60

Table of Content

A propeller type donor imparts organic solubility to oligoethylene glycol substituted conjugated small molecules. The oligoethylene glycol facilitates better intermolecular contacts and improved organic field effect transistor efficiency.